CONDENSED MATTER PHYSICS

K-Λ crossover transition in the conduction band of monolayer MoS_2 under hydrostatic pressure

Lei Fu,[1] Yi Wan,[1] Ning Tang,[1,2]* Yi-min Ding,[1] Jing Gao,[3] Jiachen Yu,[1] Hongming Guan,[1] Kun Zhang,[1] Weiying Wang,[1] Caifeng Zhang,[1] Jun-jie Shi,[1] Xiang Wu,[3] Su-Fei Shi,[4,5] Weikun Ge,[1] Lun Dai,[1,2]* Bo Shen[1,2]*

Monolayer MoS_2 is a promising material for optoelectronics applications owing to its direct bandgap, enhanced Coulomb interaction, strong spin-orbit coupling, unique valley pseudospin degree of freedom, etc. It can also be implemented for novel spintronics and valleytronics devices at atomic scale. The band structure of monolayer MoS_2 is well known to have a direct gap at K (K′) point, whereas the second lowest conduction band minimum is located at Λ point, which may interact with the valence band maximum at K point, to make an indirect optical bandgap transition. We experimentally demonstrate the direct-to-indirect bandgap transition by measuring the photoluminescence spectra of monolayer MoS_2 under hydrostatic pressure at room temperature. With increasing pressure, the direct transition shifts at a rate of 49.4 meV/GPa, whereas the indirect transition shifts at a rate of −15.3 meV/GPa. We experimentally extract the critical transition point at the pressure of 1.9 GPa, in agreement with first-principles calculations. Combining our experimental observation with first-principles calculations, we confirm that this transition is caused by the K-Λ crossover in the conduction band.

INTRODUCTION

Atomically thin transition metal dichalcogenides (TMDCs) have attracted great attention during the past few years, among which monolayer MoS_2 [a two-dimensional (2D) direct bandgap semiconductor] has been in the spotlight of 2D material research. Monolayer MoS_2 exhibits a sandwich structure with a plane of Mo atoms covalently bonded to two planes of sulfur atoms, as shown in Fig. 1A. Although multilayer and bulk MoS_2 have an indirect bandgap between Λ point in the conduction band and Γ point in the valence band due to strong coupling of p orbits of the sulfur atoms between the layers, in contrast, the monolayer MoS_2 has a direct bandgap in the visible regime (*1*, *2*), which is ideal for the exploration of optoelectronic applications. Its conduction band minimum (CBM) and valence band maximum (VBM), dominated by d orbits of Mo atoms (*3*), are located at the doubly degenerate corners (K and K′) of the hexagonal Brillouin zone. The second lowest CBM at Λ point and the second highest VBM at Γ point, as shown in Fig. 1A, are dominated by both d orbits of Mo atoms and p orbits of S atoms. The different pseudospin configurations for excitons at K and K′ valleys in monolayer MoS_2 (*4*) bring about an optical selection rule (*5*–*8*), in which the two valley states couple respectively to a σ^+ or σ^- circularly polarized photon only, as well as other novel phenomena, such as the valley Hall effect (*4*, *9*). Combining with its other unique and appealing features, such as an exceptionally large Coulomb interaction (*10*–*13*) and strong spin-orbit coupling (*14*–*16*), monolayer MoS_2 becomes a promising material for applications in optoelectronics, spintronics, and valleytronics (*17*–*19*).

Atomically thin TMDCs are also promising candidates for nanoflexible devices. Compared with bulk materials, strain will be much easier to apply in these 2D materials and will cause many effects in the applications. Applying strain and stress is a proven strategy for modulating the band structure of semiconductors (*3*, *20*–*29*), especially for semiconductors with multivalleys in the Brillouin zone. Because of different shift rates of various valleys with increasing pressure, the bandgap may change from direct to indirect or vice versa. For monolayer MoS_2, the valley effects mainly exist in the direct K-K transition; thus, it is important to clarify the relationship of the band structure versus pressure for strain-based applications. Theoretical calculations for monolayer MoS_2 result in direct-to-indirect bandgap transition under both tensile (*3*, *25*, *30*) and compressive strains (*3*, *25*, *27*, *31*) with different mechanisms. Here, tensile and compressive strain means the crystal lattice that is being enlarged or reduced, respectively. The former is thought to be caused by the transition of the VBM from K to Γ valley (*3*, *25*, *30*), whereas the latter is still controversial, because it could be due to the change of either CBM from K to Λ valley (*3*, *25*, *30*, *31*) or VBM from K to Γ valley (*27*). Referring to the aspect of experiments, although many studies (*26*–*28*, *32*, *33*) have been performed, the transition is not really seen under tensile strain, whereas it is still absent under compressive strain.

Applying hydrostatic pressure by DAC has been proven an effective approach for tuning and probing the electronic structure of semiconductors. It could vary the lattice constant and tilt the angle between the strong Mo-S bonds of monolayer MoS_2, thus altering the interaction strength between different electronic states and deforming the band structure continuously and controllably. Combining it with photoluminescence (PL) spectroscopy, which directly probes the energy of the electron-hole pairs (or excitons), one can unambiguously determine the energy shift of the electronic bands at various locations in the reciprocal space, thus demonstrating the band structure evolution by hydrostatic pressure modulating.

Here, the experimental evidence for direct-to-indirect bandgap transition of monolayer MoS_2 is observed by PL spectra under hydrostatic pressure at room temperature. With increasing pressure, the energy peak first exhibits a blue shift at a rate of 49.4 meV/GPa and then a red shift at a rate of 15.3 meV/GPa. The critical turning pressure

[1]State Key Laboratory of Artificial Microstructure and Mesoscopic Physics, School of Physics, Peking University, Beijing 100871, China. [2]Collaborative Innovation Center of Quantum Matter, Beijing 100871, China. [3]Ministry of Education Key Laboratory of Orogenic Belts and Crustal Evolution, School of Earth and Space Sciences, Peking University, Beijing 100871, China. [4]Department of Chemical and Biological Engineering, Rensselaer Polytechnic Institute, Troy, NY 12180, USA. [5]Department of Electrical, Computer, and Systems Engineering, Rensselaer Polytechnic Institute, Troy, NY 12180 USA.
*Corresponding author. Email: ntang@pku.edu.cn (N.T.); lundai@pku.edu.cn (L.D.); bshen@pku.edu.cn (B.S.)

occurs at 1.9 GPa. Combining with first-principles calculations, we can confirm that this transition comes from the change of the CBM from K to Λ valley. In addition, the energy difference at atmosphere between the K and Λ valleys in the conduction band is derived to be 118 meV.

RESULTS AND DISCUSSION

The as-grown MoS_2 sample is monolayer and uniform, which was characterized by optical microscope, atomic force microscope (AFM), and Raman spectrum, as shown in Fig. 1 (B and C). The PL was collected with a micro-PL system with pressure applied by a DAC device, as schematically shown in Fig. 1D. The PL spectra of the monolayer MoS_2 at various pressures are shown in Fig. 2A, with background signal subtracted. Here, the pressure is isotropic for the monolayer MoS_2. The Si substrate (with a layer of 300-nm SiO_2 on its surface) does not transmit an additional pressure in plane, as proved by the Raman spectra (fig. S1) shown in the Supplementary Materials. For the initial pressure at 0.9 GPa (below that pressure, the pressure calibration was not accurate), the PL peak at 1.82 eV corresponds mainly to the direct K-K transition due to its direct transition nature. The PL curves at different pressures were fitted using Lorentz function to obtain the major peak position under different pressures, as shown by black square dots in Fig. 2B. With increasing pressure, the peak energy first blue shifts and then red shifts, where a clear pressure-induced changeover of the optical bandgap occurs at approximately 1.9 GPa, indicating a direct-indirect bandgap transition.

The turnover from blue shift to red shift of the PL peak energy can be well understood, considering the effect of anticrossing of the electronic states under pressure. Pressure-induced band anticrossing behaviors have been found in III-V and II-VI semiconductors (*34*–*39*). We consider this mechanism for the analysis and take the predominant peak as the lower branch. The upper branch is hard to clarify accurately because of the large full width at half maximum at room temperature.

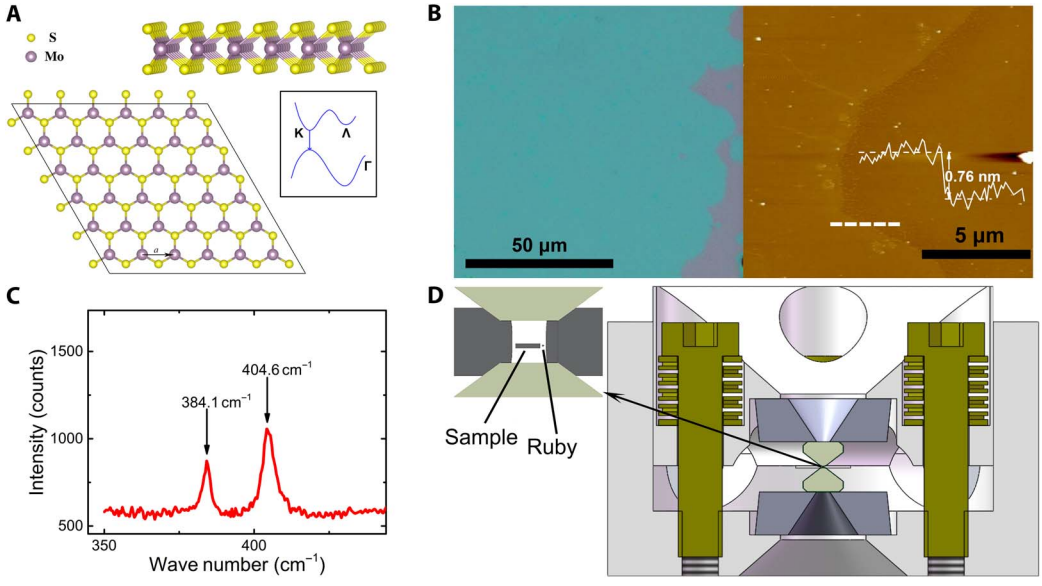

Fig. 1. Sample and technical information. (**A**) Schematic diagram of the lattice structure and band structure of monolayer MoS_2, where *a* represents the in-plane lattice constants. (**B**) The left image is the surface morphology of the as-grown sample under optical microscope. The green area is monolayer MoS_2, and pink area is the Si/SiO_2 substrate without MoS_2. The right image is the AFM image of the as-grown sample, showing that the MoS_2 is monolayer. (**C**) Raman spectra of the as-grown sample. (**D**) Schematic diagram of the diamond anvil cell (DAC) used for applying hydrostatic pressure to the sample.

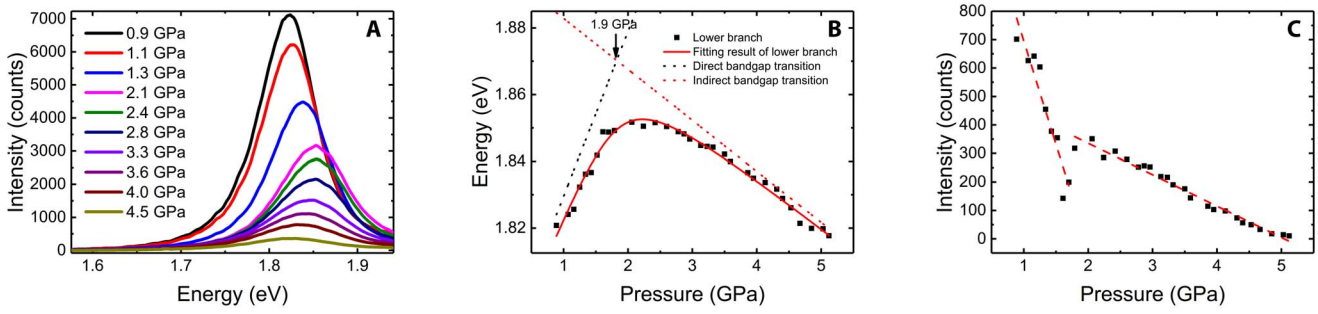

Fig. 2. Pressure-dependent PL spectra of monolayer MoS_2. (**A**) PL spectra of monolayer MoS_2 for various pressures, with background signal subtracted. (**B**) The evolution of energy of the predominant PL peak versus pressure. Black dots represent peak energies of monolayer MoS_2 under various pressures, taken as the lower branch; red solid line represents the fitting result of the lower branch; and black and red dotted lines represent the direct and indirect transition under various pressures extracted from the fitting, respectively. (**C**) Integrated intensities of PL peak under various pressures.

It is assumed that the relationship between the direct K-K transition energy and pressure obeys an equation of $E_1(p) = E_{10} + k_1 p$, where $E_1(p)$ represents the energy of K-K transition, E_{10} represents the original bandgap of the K-K transition, k_1 is the pressure rate of the transition, and p is the pressure. While the relationship between the indirect transition energy and pressure obeys a similar equation of $E_2(p) = E_{20} + k_2 p$, the anticrossing-resulted lower branch was fitted by using the following formula, taking the lower value of the equation

$$E_{\pm} = \frac{[E_{10} + E_{20} + (k_1 + k_2)p] \pm \sqrt{(E_{10} - E_{20} + (k_1 - k_2)p)^2 + 4\lambda^2}}{2} \quad (1)$$

where λ is an interaction parameter. Here, we neglect the exciton binding energy, because it is usually considered not to be affected by pressure (*32*, *40*, *41*). The result is shown as the red solid line in Fig. 2B. Through the fitting, we obtained that the energy difference at atmosphere between the K and Λ valleys in the conduction band is 118 meV, whereas the pressure coefficients are 49.4 and −15.3 meV/GPa for the direct and indirect transitions, respectively.

The integrated intensity of the PL peak under various pressures is shown in Fig. 2C. One can see that the intensity continuously decreases with pressure. This is related to electrons transferring from K to its adjacent valley in the conduction band or valence band, because the band structure gradually changes from direct to indirect with increasing pressure. Moreover, the slopes change at around 1.8 GPa, again indicating a transition of the recombination nature from direct to indirect occurring at this pressure. It is found that the intensity shows a discontinuity at the transition point. We believe that there exists a competition between the direct and indirect transition around the crossing-over point, where they have the same transition energy. The interference between them along with the anticrossing effect results in a reduction in transition probability of both transitions.

THEORETICAL CALCULATIONS

First-principles calculations are carried out to simulate the band evolution under various pressures. The relationships of direct (K-K) and indirect (Λ-K and K-Γ) bandgap versus pressure are shown in Fig. 3. The monolayer MoS_2 at atmosphere is a direct bandgap semiconductor, with both CBM and VBM located at K point, as shown in Fig. 3A. As the applied pressure increases, the K valley of the conduction band goes upward, whereas Λ valley goes downward, resulting in a crossover of the two valleys at 2.1 GPa, as shown in Fig. 3B. For pressure above 2.1 GPa, the Λ valley of the conduction band becomes lower than the K valley, as shown in Fig. 3C, resulting in an indirect bandgap. For the relationship of bandgap evolution versus pressure, Fig. 3D shows that with pressure increasing, the direct K-K gap increases, whereas the indirect Λ-K gap decreases, and the crossover point is 2.1 GPa, consistent with our experimental results. Besides, the gap between CBM at K point and VBM at Γ point is enlarged; thus, the possibility of K-Γ crossover in the valence band is excluded in the interpretation of the experimental results. This can be physically attributed to the increasing internal angle of the S–Mo–S bond under pressure (*31*). The states at the bottom of the conduction band at Λ point (BCB-Λ) and that at the top of the valence band at K point (TVB-K) make a pair of bonding and antibonding states with mainly $d_{x^2-y^2}$ and d_{xy} characters, whereas the states at BCB-K and that at TVB-Γ make a pair of states with mainly d_{z^2} character. When the bond angle

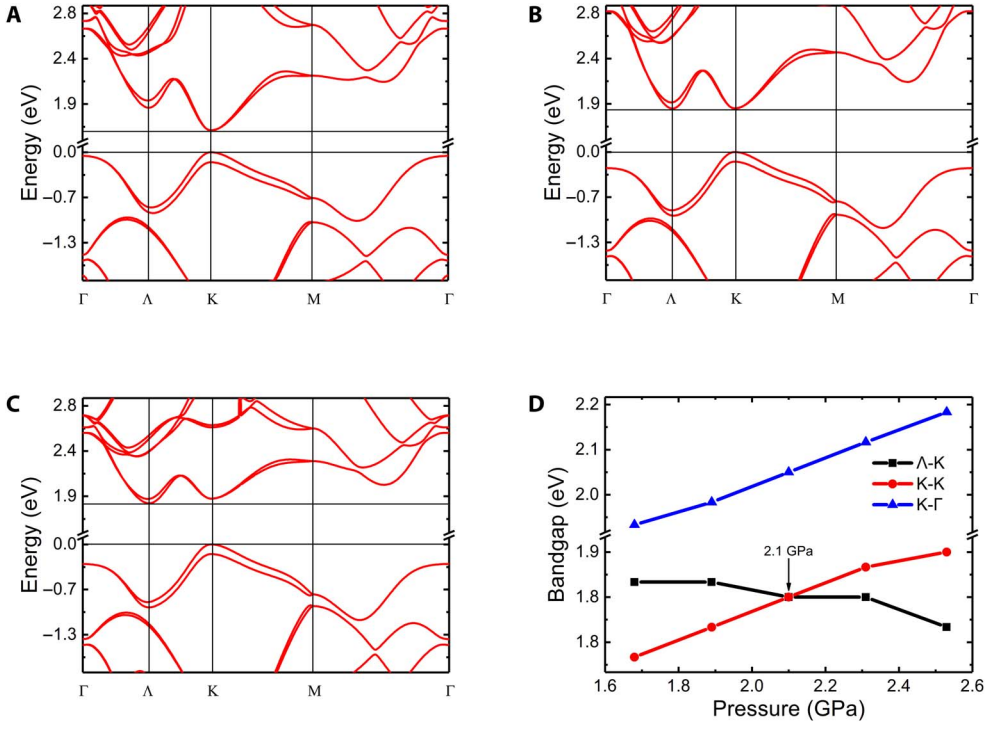

Fig. 3. First-principles calculations for the relationship of bandgap versus pressure. (**A** to **C**) are calculated band structures at 0, 2.1, and 2.5 GPa, respectively. The VBM of K point is set to be zero. (**D**) Functional relationships of bandgap versus pressure. Black, red, and blue dots represent the Λ-K, K-K, and K-Γ transitions, respectively.

increases because of applied pressure, the coupling between BCB-K and TVB-Γ strengthens, whereas that between BCB-Λ and TVB-K weakens. Thus, the energy splitting of the pair of states at BCB-K and TVB-Γ increases, whereas that at BCB-Λ and TVB-K decreases with increasing pressure. This finally results in the K-Λ crossover in the conduction band. Thus, it is confirmed that the transition that occurred in our experiments is truly due to the change of the CBM from K to Λ valley.

SUMMARY

In summary, by using hydrostatic pressure PL measurements, we experimentally demonstrate the K-Λ crossover in the conduction band in monolayer MoS_2, in agreement with theoretical calculations. With increasing pressure, the predominant PL peak exhibits first a blue shift at a rate of 49.4 meV/GPa and then a red shift at a rate of 15.3 meV/GPa, with a crossing point at 1.9 GPa, indicating a direct-indirect transition of band structure at that critical pressure. The integrated intensity of the PL peak decreases with increasing pressure at different rates, with a turning point at around 1.8 GPa, further evidencing our observation of the critical point of transition. In addition, first-principles calculations are carried out to simulate the band structure of monolayer MoS_2 at different pressures, resulting in a K-Λ crossover in the conduction band occurring with increasing pressure, with the turning point at 2.1 GPa, consistent with our experimental observation. We therefore conclude that the direct-indirect bandgap transition under hydrostatic pressure originates from the K-Λ crossover in the conduction band of monolayer MoS_2.

Different from the direct-to-indirect transition from monolayer to multilayer TMDCs (mainly caused by increasing interlayer coupling), the transition occurring under pressure for monolayer MoS_2 is caused by the pressure-induced K-Λ crossover transition in the conduction band. Because of the lack of interlayer coupling in monolayer MoS_2, this transition mechanism is an intrinsic intralayer nature, which is only related to the interaction of atoms within a monolayer. Moreover, this conclusion may be extended to other semiconductors, especially those with multivalleys in the Brillouin zone, such as other monolayer TMDCs (WS_2, $MoTe_2$, etc.), owing the same crystal structure and similar band structure with monolayer MoS_2.

MATERIALS AND METHODS

Sample fabrication

Monolayer MoS_2 was grown by a chemical vapor deposition method in a dual-temperature zone system using S (99.999%; Ourchem) and MoO_3 (99.99%; Ourchem) as sources, perylene-3,4,9,10-tetracarboxylic acid tetrapotassium salt as a seeding promoter, pieces of prethinned Si substrate with a layer of 300-nm SiO_2 on its surface as substrates, and high-purity inert argon as carrier gas. The layer number of the as-grown MoS_2 was identified by optical microscope and micro-Raman measurement.

Experimental setup

Micro-PL measurements were carried out at room temperature with a microscope imaging system. A continuous-wave laser with wavelength of 532 nm and stable power of 10 mW was focused on the sample in a DAC device by a long working distance objective (50×; numerical aperture, 0.35), and the focus spot size was about 7 μm. In the experiment, the laser power below 18 mW is safe for the sample. The PL signal from the sample was collected by the same objective and then sent to a HORIBA iHR550 spectrometer, where the final detection was carried out by a liquid nitrogen–cooled charge-coupled device. The data acquisition time of the PL measurements is 1 s. The pressure was applied by a DAC device with 300-μm diameter of culets. Silicone oil was used as the pressure-transmitting medium, and the pressure was determined by the shift of the R1 fluorescence line of ruby at alongside of the sample.

First-principles calculations

Our first-principles calculations were performed by using density functional theory in the generalized gradient approximation with Perdew-Burke-Ernzerhof functional for electron exchange and correlation potentials, as implemented in the Vienna Ab initio Simulation Package (*42*–*44*). The 4p, 4d, and 5s electrons of Mo atom and 3s and 3p electrons of S atom were treated as the valence electrons. The electron-ion interaction was described by using the projector augmented-wave method, and the energy cutoff was set to 500 eV. The structures were fully optimized by using the conjugate gradient algorithm until the maximum energy difference and residual atomic forces converge to 10^{-4} eV and 0.01 eV/Å, respectively. A well-converged Monkhorst-Pack k-point set of 21 × 21 × 1 was adopted, and a vacuum layer larger than 20 Å was used to ensure the decoupling between the periodically repeated cells. The spin-orbit interaction was included in our calculations.

SUPPLEMENTARY MATERIALS

Supplementary material for this article is available at http://advances.sciencemag.org/cgi/content/full/3/11/e1700162/DC1

fig. S1. Raman spectra of monolayer MoS_2 under various pressures.

References (*45*, *46*)

REFERENCES AND NOTES

1. K. F. Mak, C. Lee, J. Hone, J. Shan, T. F. Heinz, Atomically thin MoS_2: A new direct-gap semiconductor. *Phys. Rev. Lett.* **105**, 136805 (2010).
2. A. Splendiani, L. Sun, Y. Zhang, T. Li, J. Kim, C. Y. Chim, G. Galli, F. Wang, Emerging photoluminescence in monolayer MoS_2. *Nano Lett.* **10**, 1271–1275 (2010).
3. C.-H. Chang, X. Fan, S.-H. Lin, J.-L. Kuo, Orbital analysis of electronic structure and phonon dispersion in MoS_2, $MoSe_2$, WS_2, and WSe_2 monolayers under strain. *Phys. Rev. B* **88**, 195420 (2013).
4. D. Xiao, G.-B. Liu, W. Feng, X. Xu, W. Yao, Coupled spin and valley physics in monolayers of MoS_2 and other group-VI dichalcogenides. *Phys. Rev. Lett.* **108**, 196802 (2012).
5. T. Cao, G. Wang, W. Han, H. Ye, C. Zhu, J. Shi, Q. Niu, P. Tan, E. Wang, B. Liu, J. Feng, Valley-selective circular dichroism of monolayer molybdenum disulphide. *Nat. Commun.* **3**, 887 (2012).
6. A. M. Jones, H. Yu, N. J. Ghimire, S. Wu, G. Aivazian, J. S. Ross, B. Zhao, J. Yan, D. G. Mandrus, D. Xiao, W. Yao, X. Xu, Optical generation of excitonic valley coherence in monolayer WSe_2. *Nat. Nanotechnol.* **8**, 634–638 (2013).
7. K. F. Mak, K. He, J. Shan, T. F. Heinz, Control of valley polarization in monolayer MoS_2 by optical helicity. *Nat. Nanotechnol.* **7**, 494–498 (2012).
8. H. Zeng, J. Dai, W. Yao, D. Xiao, X. Cui, Valley polarization in MoS_2 monolayers by optical pumping. *Nat. Nanotechnol.* **7**, 490–493 (2012).
9. K. F. Mak, K. L. McGill, J. Park, P. L. McEuen, The valley Hall effect in MoS_2 transistors. *Science* **344**, 1489–1492 (2014).
10. K. F. Mak, K. He, C. Lee, G. H. Lee, J. Hone, T. F. Heinz, J. Shan, Tightly bound trions in monolayer MoS_2. *Nat. Mater.* **12**, 207–211 (2013).
11. A. Ramasubramaniam, Large excitonic effects in monolayers of molybdenum and tungsten dichalcogenides. *Phys. Rev. B* **86**, 115409 (2012).
12. M. M. Ugeda, A. J. Bradley, S.-F. Shi, F. H. da Jornada, Y. Zhang, D. Y. Qiu, W. Ruan, S.-K. Mo, Z. Hussain, Z.-X. Shen, F. Wang, S. G. Louie, M. F. Crommie, Giant bandgap renormalization and excitonic effects in a monolayer transition metal dichalcogenide semiconductor. *Nat. Mater.* **13**, 1091–1095 (2014).
13. Z. Ye, T. Cao, K. O'Brien, H. Zhu, X. Yin, Y. Wang, S. G. Louie, X. Zhang, Probing excitonic dark states in single-layer tungsten disulphide. *Nature* **513**, 214–218 (2014).
14. A. Molina-Sánchez, D. Sangalli, K. Hummer, A. Marini, L. Wirtz, Effect of spin-orbit interaction on the optical spectra of single-layer, double-layer, and bulk MoS_2. *Phys. Rev. B* **88**, 045412 (2013).

15. L. Sun, J. Yan, D. Zhan, L. Liu, H. Hu, H. Li, B. K. Tay, J.-L. Kuo, C.-C. Huang, D. W. Hewak, P. S. Lee, Z. X. Shen, Spin-orbit splitting in single-layer MoS_2 revealed by triply resonant Raman scattering. *Phys. Rev. Lett.* **111**, 126801 (2013).
16. Z. Y. Zhu, Y. C. Cheng, U. Schwingenschlögl, Giant spin-orbit-induced spin splitting in two-dimensional transition-metal dichalcogenide semiconductors. *Phys. Rev. B* **84**, 153402 (2011).
17. R. S. Sundaram, M. Engel, A. Lombardo, R. Krupke, A. C. Ferrari, Ph. Avouris, M. Steiner, Electroluminescence in single layer MoS_2. *Nano Lett.* **13**, 1416–1421 (2013).
18. O. Lopez-Sanchez, D. Lembke, M. Kayci, A. Radenovic, A. Kis, Ultrasensitive photodetectors based on monolayer MoS_2. *Nat. Nanotechnol.* **8**, 497–501 (2013).
19. B. Radisavljevic, A. Radenovic, J. Brivio, V. Giacometti, A. Kis, Single-layer MoS_2 transistors. *Nat. Nanotechnol.* **6**, 147–150 (2011).
20. Z.-H. Chi, X.-M. Zhao, H. Zhang, A. F. Goncharov, S. S. Lobanov, T. Kagayama, M. Sakata, X.-J. Chen, Pressure-induced metallization of molybdenum disulfide. *Phys. Rev. Lett.* **113**, 036802 (2014).
21. O. Kohulák, R. Martoňák, E. Tosatti, High-pressure structure, decomposition, and superconductivity of MoS_2. *Phys. Rev. B* **91**, 144113 (2015).
22. A. P. Nayak, S. Bhattacharyya, J. Zhu, J. Liu, X. Wu, T. Pandey, C. Jin, A. K. Singh, D. Akinwande, J.-F. Lin, Pressure-induced semiconducting to metallic transition in multilayered molybdenum disulphide. *Nat. Commun.* **5**, 3731 (2014).
23. Q. Zhang, Y. Cheng, L.-Y. Gan, U. Schwingenschlögl, Giant valley drifts in uniaxially strained monolayer MoS_2. *Phys. Rev. B* **88**, 245447 (2013).
24. T. Cheiwchanchamnangij, W. R. L. Lambrecht, Y. Song, H. Dery, Strain effects on the spin-orbit-induced band structure splittings in monolayer MoS_2 and graphene. *Phys. Rev. B* **88**, 155404 (2013).
25. W. S. Yun, S. W. Han, S. C. Hong, I. G. Kim, J. D. Lee, Thickness and strain effects on electronic structures of transition metal dichalcogenides: 2H-MX_2 semiconductors (M=Mo, W;X=S, Se, Te). *Phys. Rev. B* **85**, 033305 (2012).
26. H. J. Conley, B. Wang, J. I. Ziegler, R. F. Haglund Jr., S. T. Pantelides, K. I. Bolotin, Bandgap engineering of strained monolayer and bilayer MoS_2. *Nano Lett.* **13**, 3626–3630 (2013).
27. A. P. Nayak, T. Pandey, D. Voiry, J. Liu, S. T. Moran, A. Sharma, C. Tan, C.-H. Chen, L.-J. Li, M. Chhowalla, J.-F. Lin, A. K. Singh, D. Akinwande, Pressure-dependent optical and vibrational properties of monolayer molybdenum disulfide. *Nano Lett.* **15**, 346–353 (2015).
28. C. R. Zhu, G. Wang, B. L. Liu, X. Marie, X. F. Qiao, X. Zhang, X. X. Wu, H. Fan, P. H. Tan, T. Amand, B. Urbaszek, Strain tuning of optical emission energy and polarization in monolayer and bilayer MoS_2. *Phys. Rev. B* **88**, 121301 (2013).
29. H. Peelaers, C. G. Van de Walle, Effects of strain on band structure and effective masses in MoS_2. *Phys. Rev. B* **86**, 241401 (2012).
30. E. Scalise, M. Houssa, G. Pourtois, V. Afanas'ev, A. Stesmans, Strain-induced semiconductor to metal transition in the two-dimensional honeycomb structure of MoS_2. *Nano Res.* **5**, 43–48 (2011).
31. X. Fan, C.-H. Chang, W. T. Zheng, J.-L. Kuo, D. J. Singh, The electronic properties of single-layer and multilayer MoS_2 under high pressure. *J. Phys. Chem. C* **119**, 10189–10196 (2015).
32. K. He, C. Poole, K. F. Mak, J. Shan, Experimental demonstration of continuous electronic structure tuning via strain in atomically thin MoS_2. *Nano Lett.* **13**, 2931–2936 (2013).
33. X. Dou, K. Ding, D. Jiang, B. Sun, Tuning and identification of interband transitions in monolayer and bilayer molybdenum disulfide using hydrostatic pressure. *ACS Nano* **8**, 7458–7464 (2014).
34. G. H. Li, A. R. Goñi, K. Syassen, O. Brandt, K. Ploog, State mixing in InAs/GaAs quantum dots at the pressure-induced Γ-X crossing. *Phys. Rev. B* **50**, 18420–18425 (1994).
35. T. Mattila, S.-H. Wei, A. Zunger, Localization and anticrossing of electron levels in $GaAs_{1-x}N_x$ alloys. *Phys. Rev. B* **60**, R11245–R11248 (1999).
36. W. Shan, W. Walukiewicz, J. W. Ager III, E. E. Haller, J. F. Geisz, D. J. Friedman, J. M. Olson, S. R. Kurtz, Band anticrossing in GaInNAs alloys. *Phys. Rev. Lett.* **82**, 1221–1224 (1999).
37. W. Walukiewicz, W. Shan, K. M. Yu, J. W. Ager III, E. E. Haller, I. Miotkowski, M. J. Seong, H. Alawadhi, A. K. Ramdas, Interaction of localized electronic states with the conduction band: Band anticrossing in II-VI semiconductor ternaries. *Phys. Rev. Lett.* **85**, 1552–1555 (2000).
38. J. Wu, W. Shan, W. Walukiewicz, K. M. Yu, J. W. Ager III, E. E. Haller, H. P. Xin, C. W. Tu, Effect of band anticrossing on the optical transitions in $GaAs_{1-x}N_x$/GaAs multiple quantum wells. *Phys. Rev. B* **64**, 085320 (2001).
39. J. Wu, W. Walukiewicz, K. M. Yu, J. W. Ager III, E. E. Haller, Y. G. Hong, H. P. Xin, C. W. Tu, Band anticrossing in $GaP_{1-x}N_x$ alloys. *Phys. Rev. B* **65**, 241303 (2002).
40. H. Shi, H. Pan, Y.-W. Zhang, B. I. Yakobson, Quasiparticle band structures and optical properties of strained monolayer MoS_2 and WS_2. *Phys. Rev. B* **87**, 155304 (2013).
41. J. Feng, X. Qian, C.-W. Huang, J. Li, Strain-engineered artificial atom as a broad-spectrum solar energy funnel. *Nat. Photonics* **6**, 866–872 (2012).
42. G. Kresse, J. Furthmüller, Efficiency of ab-initio total energy calculations for metals and semiconductors using a plane-wave basis set. *Comput. Mater. Sci.* **6**, 15–50 (1996).
43. G. Kresse, J. Hafner, *Ab initio* molecular dynamics for liquid metals. *Phys. Rev. B* **47**, 558–561 (1993).
44. G. Kresse, D. Joubert, From ultrasoft pseudopotentials to the projector augmented-wave method. *Phys. Rev. B* **59**, 1758–1775 (1999).
45. M. A. Hopcroft, W. D. Nix, T. W. Kenny, What is the young's modulus of silicon? *J. Microelectromech. Syst.* **19**, 229–238 (2010).
46. N. Bandaru, R. S. Kumar, D. Sneed, O. Tschauner, J. Baker, D. Antonio, S.-N. Luo, T. Hartmann, Y. Zhao, R. Venkat, Effect of pressure and temperature on structural stability of MoS_2. *J. Phys. Chem. C* **118**, 3230–3235 (2014).

Acknowledgments

Funding: This work was supported by the National Basic Research Program of China (no. 2013CB921901), and the National Natural Science Foundation of China (nos. 61376095, 61522401, 61574006, 61521004, 11634002, 11474007, 11474012, and 61361166007).

Author contributions: N.T. and L.D. conceived the project. Y.W., K.Z., and L.D. grew and characterized the monolayer MoS_2 films. L.F., J.G., J.Y., and X.W. fabricated the DAC samples. L.F., H.G., C.Z., and W.W. performed the PL measurements under hydrostatic pressure. Y.-m.D. and J.-j.S. performed the theoretical calculations. L.F. and J.Y. carried out the data analysis. L.F., Y.W., N.T., L.D., S.-F.S., and W.G. wrote the manuscript. N.T., L.D., W.G., and B.S. guided the research. All authors discussed the results and commented on the manuscript. **Competing interests:** The authors declare that they have no competing interests. **Data and materials availability:** All data needed to evaluate the conclusions in the paper are present in the paper and/or the Supplementary Materials. Additional data related to this paper may be requested from the authors.

Submitted 16 January 2017
Accepted 6 October 2017
Published 3 November 2017
10.1126/sciadv.1700162

Citation: L. Fu, Y. Wan, N. Tang, Y.-. Ding, J. Gao, J. Yu, H. Guan, K. Zhang, W. Wang, C. Zhang, J.-. Shi, X. Wu, S.-F. Shi, W. Ge, L. Dai, B. Shen, K-Λ crossover transition in the conduction band of monolayer MoS_2 under hydrostatic pressure. *Sci. Adv.* **3**, e1700162 (2017).

ScienceAdvances

K-Λ crossover transition in the conduction band of monolayer MoS_2 under hydrostatic pressure

Lei Fu, Yi Wan, Ning Tang, Yi-min Ding, Jing Gao, Jiachen Yu, Hongming Guan, Kun Zhang, Weiying Wang, Caifeng Zhang, Jun-jie Shi, Xiang Wu, Su-Fei Shi, Weikun Ge, Lun Dai and Bo Shen

Sci Adv **3** (11), e1700162.
DOI: 10.1126/sciadv.1700162